Photometric Method in Energy Determination of Cosmic-Ray Showers in Emulsion Chamber

Itaru OHTA

Institute for Nuclear Study, University of Tokyo, Tokyo

(Received December 24, 1970)

Since Japan-Brazil Emulsion Chamber Collaboration started in 1962 on Mt. Chacaltaya, X-ray films have been used together with nuclear emulsion plates for detection of the high energy cosmic-ray showers. Meanwhile, many members, Japanese and Brazilians, of this collaboration have made various attempts to use X-ray film for energy determination as well as for detection. The present work is developed in this basis.

Application of the photometric method with X-ray films for energy determination of high energy electron showers gives us the following advantages. Firstly, signal to noise ratio of shower spot on X-ray film is much higher than that on nuclear emulsion plate, because of high sensitivity of X-ray films. Secondly, measurement of spot darkness of shower using micro-densitometer is more facile and more rapid, as compared with counting of electron tracks of the shower in nuclear emulsion plates. Consequently, the photometric method with X-ray film enabled us to make a scale-up of emulsion chamber with great stride.

Photometric measurement and track counting method are applied simultaneously to each of 47 showers and the correspondence between spot darkness, D_{max}, and shower energy, E_0, is established empirically. The relation is also calculated with three-dimensional shower theory. Both results agree well and give the relation $D_{max} \propto E_0^{0.85}$ for various energies.

The method of energy determination for localized nuclear interaction in the chamber itself—Pb-jet shower—is also established empirically and theoretically. The same method as for electron shower is valid for Pb-jet showers with energy $\Sigma E_r \gtrsim 1$ TeV, if one uses slit larger than 150 μm radius in micro-densitometer.

§1. Introduction

The emulsion chamber consists of many layers of lead plates interposed with layers of photo-sensitive material—nuclear emulsion plates, N-type and RR-type X-ray films—sometimes together with artificial jet producer and free space. It has been developed in Japan since the balloon flight project in 1956, and it is recognized at present as one of the most suitable apparatuses for study of high energy phenomena by its accuracy in energy determination and space resolution.[1)]

When a cosmic-ray particle of the electromagnetic component comes into the emulsion chamber, it produces an electron shower in the chamber. One can determine its energy by measuring the size of the electron shower by using photo-sensitive material. The same method can be applied to showers from the local nuclear interaction in the chamber itself. In practice, the energy measurement has been made by counting the number of the shower tracks

recorded in nuclear emulsion plates in the chamber. A transition curve of the number of shower tracks within a circle of a certain radius (usually 50 μm for TeV energy regions) is constructed and compared with the theoretical values calculated from the three-dimensional shower theory.[2),3)]

When the energy exceeds a few TeV, denstiy of the shower tracks near the center becomes so high that one can no longer separate and count individual tracks of the shower. To avoid the above difficulty, the method of counting was revised to measure the number of shower tracks within an annular ring having radius between 12.5 μm and 50 μm around the center. And for the highest energy cases, say with energy greater than 10 TeV, a measurement was made on lateral distribution of the shower tracks and the results were compared with corresponding theoretical values calculated from the three-dimensional shower theory to determine the energy.[3)] With those methods, however, one needs a great deal of efforts under microscope for energy determination.

A photometric method has been developed for energy determination of high energy showers in order to avoid these difficulties of the track counting method. In the emulsion chamber, two kinds of industrial X-ray film, Sakura N-type and RR-type, are compiled just above a nuclear emulsion plate. A shower with a size over a certain value produces a dark spot on the X-ray film, which can be detected by naked eye scanning. The size of the dark spot on the X-ray film depends on the shower size, thus reflecting its energy. Quantitatively, one can apply the photometric measurement of the dark spot for the energy determination. The photometric method is more convenient in practice particularly in the high energy regions.

The first of our photometric methods was to use a relation between the size of the dark spot on N-type film and the shower energy E_0. If one defines the size of a spot by the radius r_0 of the area in N-type film with darkness above a certain value, the proportional relation, $r_0 \propto E_0$, is confirmed.[4)] But the method is difficult to be applied to low energy events because of low signal to noise ratio of the films. Then, we developed another photometric method to measure directly opacity of the dark spot with a fixed aperture of the photometry apparatus. Since exposure of emulsion chamber in 1964 at Mt. Chacaltaya Laboratory, the measurement of spot darkness by microphotometer has been widely applied for energy determination of high energy γ-rays, electrons and electron showers produced by local interactions in the chamber itself. These development made scale-up of the experiment possible.

In this paper, we describe the photometric method for N-type film used in emulsion chambers. The relation between the spot darkness and the shower energy is discussed in detail compared with the results of track counting method. Moreover, it will be shown that the photometric method gives the results with high accuracy if the measurements are performed in the appro-

priate conditions taking into account the influences of development condition of films, background tracks suffered during exposure period, and inclination effect of shower incidence.

In the case of Pb-jet shower, the lateral distribution is different from that of a single electron shower because of the effect of transverse momenta of γ-rays in the nuclear interaction. The lateral distribution of Pb-jet shower can be obtained by superposing the lateral distributions of a single γ-ray. In the energy region above a few TeV, it is shown that the same method of photometry can be applicable for Pb-jet shower if one adopts the slit width sufficiently large.

§2. Fundamentals in our photometric method

2-1 *Cosmic-ray showers in emulsion chamber*

A unit of sensitive layer in the emulsion chamber usually consists of one nuclear emulsion plate (Fuji ET7A) and three X-ray films (two Sakura N-type films and one Sakura RR-type film). Table I gives specifications of the above photographic material used in the emulsion chamber. After exposure for about one year, emulsion chambers are disassembled and emulsion plates and X-ray films are processed for the development with the following procedure.

Processing routine for nuclear emulsion plates, ET7A, 50 μm

Development temperature	20 ± 0.5°C
Development time	20 min
Chemicals	amidol

Processing routine for N- and RR-type films

Development temperature	20 ± 0.5°C
Development time	15 min
Chemicals	Konidol-X

After finding dark spots in the X-ray films by naked eye scanning, the corresponding shower tracks in the emulsion plates are confirmed under a microscope. Photograph 1 shows an example of a shower recorded in nuclear

Table I. Specifications of the sensitive materials used in our emulsion chamber.

Type of emulsion	Emulsion thickness (microns)	Grain size** (microns²)	Grain size after development (microns²)	Base thickness (microns)
N-type	30	3	25	200
RR-type	25	0.5	1.6	200
ET7A*	50	0.07	0.7	1600

* Emulsion coated only on one side of a base.

** If we assume distribution of the cross-sectional area as $s\exp(-s/s_0)ds$, the average grain size cited here correponds to $2s_0$.

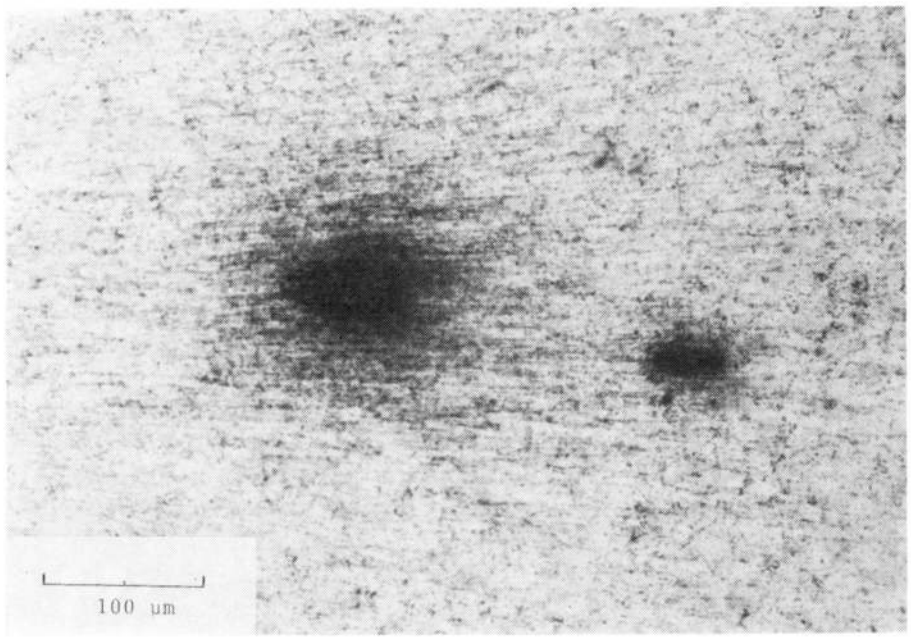

Photograph 1-a). A pair of high energy cascade showers, d-group, observed in nuclear emulsion plate. Nine high energy electron showers are also observed outside of this view. The shower corresponds to a pair of high energy γ-rays with energy of 5.3 and 3.5×10^{13} eV each.

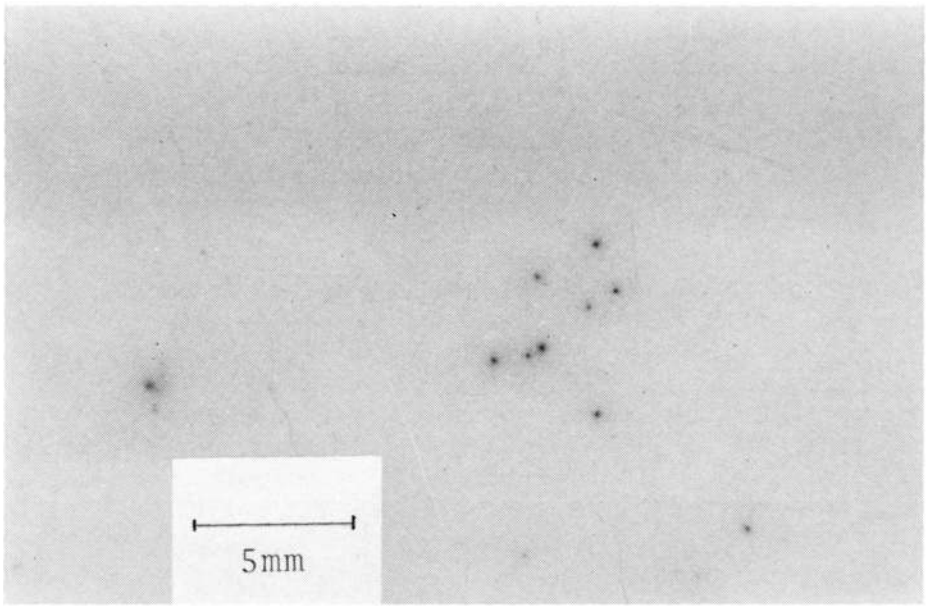

Photograph 1-b). High energy atmospheric jet, event 18-I, observed in the N-type X-ray film. The total energy of the event was estimated by the spot darkness on X-ray film as 200 TeV and the height of primary acts is estimated by 2γ-π^0 coupling method as about 200 m above the chamber.

emulsion plate, ET7A, and X-ray film, N-type. Every detected shower event is followed through the chamber as far as possible, and one makes a map of the events in each block of the chamber. Then, the X-ray films are ready for the photometry measurement and the nuclear emulsion plates for the track counting measurement.

2-2 *Instrument for photometry and measurement of spot darkness*

The micro-densitometer used in our experiments is schematically shown in Fig. 1. Light from a source lamp L is divided into two beams, S and X, which are alternately interrupted by a chopper CH. An image of the first slit S_1 is made by a condenser lens $O_1(\times 10)$ on a X-ray film to be measured. An objective lens O_2 $(\times 10)$ forms an enlarged image of the illuminated film at position of the second slit S_2. The illuminated area on the film is adjustable by the first slit S_1 up to maximum width 800 μm according to a purpose of the experiments. The second slit S_2 is adjusted to coincide with an image of the area illuminated through the slit S_1. Since numerical aperture of the condenser lens O_1 and of the objective lens O_2 is 0.25, aperture angle of the illumination is always 30°. Intensity of the separated beam X is defined by a variable aperture VA, which is automatically controlled by a feed-back loop consisting of a photo-multiplier P, an amplifier A, a balancing motor M and a cam CM so as to balance the transmitted intensity of the two beams S and X. The cam has such curvature that the rotating angle is directly proportional to logarithm of the aperture VA. The rotating angle is recorded on a recording paper automatically.

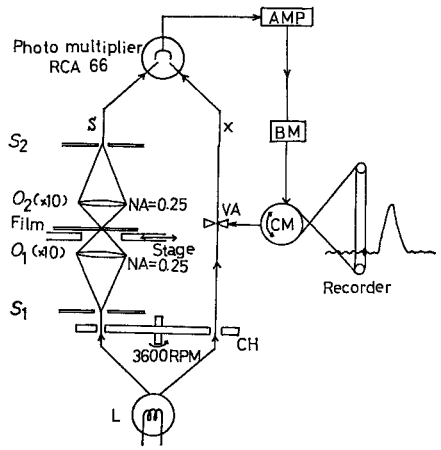

Fig. 1. Schematic illustration of micro-densitometer in our experiment.

Let J_0 be the incident light flux and J the transmitted light flux through an illuminated area of the X-ray film. Then the darkness of the concerned area of the film is given by

$$D=\log_{10} J_0/J. \tag{1}$$

The X-ray film has general background which is originated from irradiation of background radiation, chemical fog and so on. Magnitude of the background darkness, $D(\mathrm{bg})$, is usually 0.5~1.0. It depends on conditions of the exposure and also of the processing. It is found that fluctuation of the back-

ground darkness in one sheet of X-ray film is small and negligible. (See Appendix 1 for detailed discussion on the background.)

An electron shower produced by a high energy cosmic-ray particle is recorded as a small dark spot over uniform background of the film. The darkness of a shower spot is measured by the micro-densitometer illuminating the spot region of the X-ray film. Net darkness of the shower spot is obtained as a difference between the observed darkness, $D(\mathrm{ob})$, and the background darkness, $D(\mathrm{bg})$,

$$D(\mathrm{net}) = D(\mathrm{ob}) - D(\mathrm{bg}). \tag{2}$$

We will call hereafter the net darkness of a shower spot simply as the spot darkness.

The value of the spot darkness of the same spot varies with the size of the illuminated area on the spot, i.e., the size of the slit of the micro-densitometer. The micro-densitometer measurement on the shower spot is usually made with slit of a circle with 125 μm radius or of a square of 200 μm $\times$ 200 μm, both of which are equivalent to a circle with 150 μm radius, with parallel illuminating beam after correction of the numerical aperture of the lenses. For measurement of higher energy showers and locally produced showers, a larger slit size is applied.

A sheet of X-ray film is placed at the micro-densitometer so as to make the center of the slit pass through the center of the shower spot during automatic motion of its stage. An example of recording of the micro-densitometer is presented in Fig. 2, where the X-axis shows the motion of the stage of the micro-densitometer and the Y-axis observed values of the darkness. The background darkness, $D(\mathrm{bg})$, is usually measured in a region of the X-ray film about 1 cm apart from each shower spot.

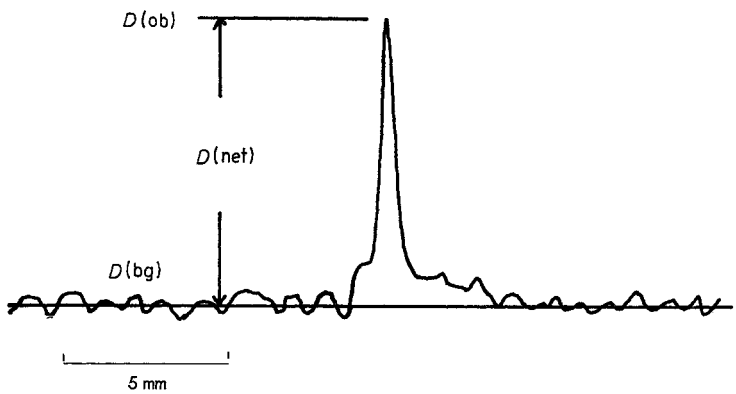

Fig. 2. An example of recording of measurement of spot darkness. $D_{max}=0.46$, $E_0=5.0$ TeV.

2-3 *Characteristics of N-type X-ray film*

In order to obtain a relation between the electron density ρ and the darkness of the N-type X-ray film, the films were exposed to the electron beam with momentum 650 MeV/c of INS electron synchrotron with various amounts of irradiation.[5] The condition of processing, different from the routine, was the following: the temperature and developing time 27.5°C and 45 sec. for N-type film and 27°C and 75 sec. for RR-type film with Konidol-X. The experimental result given in Fig. 3 shows that the darkness is proportional to the electron density up to 10^7 electrons/cm^2. One finds that the following empirical formula represents well the experimental data over the whole observed range of electron density,

$$D=D_0(1-e^{-\alpha\rho}), \tag{3}$$

where D_0 is the maximum darkness of the film and equal to about 7.0 for our case. The set of values of the parameters, D_0 and α in Eq. (3), which connect the darkness D and the electron density ρ, depends on the condition of the exposure and of the development process (chemicals, time and temperature). Accordingly, darkness of a shower spot with a certain energy will be different for different chambers. Therefore, calibration of the relation between the shower energy and the spot darkness must be done carefully in each exposure.

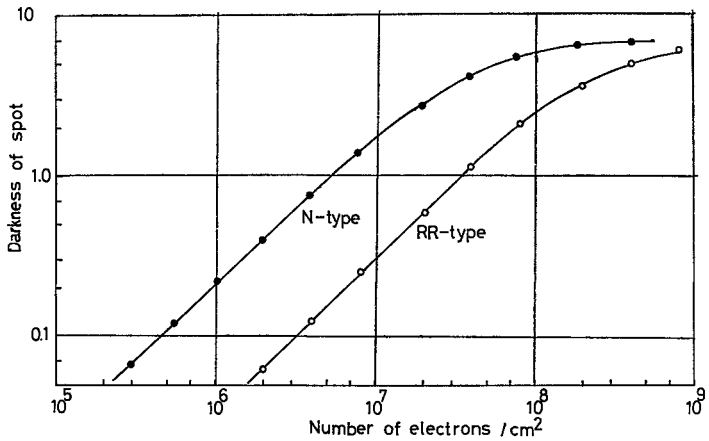

Fig. 3. Relation between the darkness of film and the density of electrons for two types of X-ray film, N and RR. Films are irradiated by electron beam with momentum 600 MeV/c from electron synchrotron.

2-4 *Characteristics of RR-type X-ray film*

The same electron beam from INS electron synchrotron was made to irradiate the RR-type films, as was made for the N-type film. The result is also presented in Fig. 3 and shows again that a linear relation holds between D and ρ up to about 10^8 electrons/cm^2. One finds here, too, that the empirical

formula, Eq. (3), represents well the experimental data over the whole observed range of the electron density. The value of D_0 in Eq. (3), the maximum darkness, is about 8.5 in this case.

When one makes a comparison of the darkness in N-type film and RR-type film, the result shows that the ratio, D_N/D_{RR}, for the same irradiation is about 6.0 in the region where a linear relation holds between D and ρ.*)

2-5 *Characteristic curve*

The relation (3) between the darkness D and the electron density ρ is called a characteristic curve of the X-ray film. That functional form of the empirical relation can be derived from the following argument with a simple model of photographic emulsion.

Let us consider a case where the beam of electrons with density ρ irradiates the X-ray film which contains n_0 silver-halide crystals per unit volume in its emulsion layer. We assume that a silver-halide crystal has a dimension of its cross-section being s and it forms a latent image when it is hitted by a single electron. Then, the sensitized grain density n can be written as follows:

$$n=n_0(1-e^{-s\rho}). \tag{4}$$

Since the darkness of film D should be proportional to density of the developed silver grains, which is equal to n, one can express the darkness as follows:

$$D(\rho)=D_0(1-e^{-s\rho}). \tag{5}$$

The parameter α in the empirical relation (3) is found to correspond to cross-sectional area of a grain, s, in this model.

§3. Energy determination of electron shower

3-1 *Spot darkness and the cascade shower theory*

Darkness of a shower spot recorded on X-ray film is determined by the lateral distribution of the shower particles, the characteristic curve of the X-ray film, and condition of the micro-densitometer measurement. We will discuss the problem for a case where a single γ-ray (or an electron) with energy E_0 comes into the emulsion chamber with the vertical direction and generates an electron shower in the chamber.

Suppose a micro-densitometer measurement is carried out for a shower spot on a X-ray film placed at depth t of an emulsion chamber. Its slit is assumed of circular shape with radius R and the center is located in coin-

*) Spot darkness for the same shower is measured for N-type and RR-type films in the emulsion chamber exposed on Mt. Chacaltaya and the result is $D_N/D_{RR}\simeq 2$. The discrepancy can be caused by the difference of conditions of exposure and processing of films (time, temperature and chemicals of development). Darkness of RR-type film is specially sensitive on such conditions.

cidence with the position of the shower center. From the above mentioned characteristic curve of X-ray film, Eq. (3), which connects the darkness and the particle density, one can define the local darkness, $d(r)$, on the infinitesimal area, $rdrd\varphi$, in the spot region at distance r from the shower center as

$$d(E_0, t, r) = D_0(1 - \exp[-\alpha\rho(E_0, t, r)]), \tag{6}$$

where $\rho(E_0, t, r)$ is density of shower electrons of the area, which is a function of distance r from the shower center, the incident energy E_0 and the depth t. Now, intensity of the transmitted light, dI, through the area $rdrd\varphi$ is written as

$$dI = I_0 \exp[-d(E_0, t, r)]rdrd\varphi, \tag{7}$$

where I_0 is intensity of the incident light.

Total flux of the transmitted light through the circular slit on the shower spot is expressed by the following integral,

$$J = 2\pi I_0 \int_0^R rdr \exp[-2.3d(E_0, t, r)], \tag{8}$$

where the incident flux J_0 is $\pi R^2 I_0$.

Therefore, the spot darkness through the slit with radius R is expressed as

$$D(E_0, t, R) = -\log_{10}\frac{2}{R^2}\int_0^R rdr \exp[-2.3d(E_0, t, r)]. \tag{9}$$

If one knows beforehand numerical values of the density of shower particles, $\rho(E_0, t, r)$, then one can calculate expected values of the spot darkness for various parameter values of E_0, t and R.

Before going into the numerical integration, we will discuss general property of the spot darkness, $D(E_0, t, R)$, with help of the electron shower theory. As is well known, the lateral distribution of electrons near the shower axis has an approximate expression as

$$\rho(E_0, t, r) \sim (E_0 \cdot r/K)^s \cdot 1/r^2 \quad \text{for} \quad r/r_1 \ll 1, \tag{10}$$

where K is the scattering constant, 19.7 MeV, r_1 is the Molière unit, 19.5 g/cm^2 in lead and s is an age parameter of the electron shower. Approximation here adopted will be called hereafter small radius approximation. The slit radius in our experiment is available up to 400 μm. This means that the illuminated area at the maximum slit radius is equivalent to $R/r_1 \simeq 7 \times 10^{-3}$, so that the small radius approximation holds in our experiment.

Let us apply the above consideration to the spot darkness at the shower maximum. One defines the maximum spot darkness, $D_{max}(E_0, R)$, as the maximum value in a transition curve of the spot darkness of a shower. For

computing $D_{max}(E_0, R)$ by Eq. (9), one may utilize small radius approximation for the lateral distribution at the shower maximum, $t=t_{max}$, which gives

$$\rho(E_0, t_{max}, r) \sim \text{const. } E_0/r. \tag{11}$$

Therefore the local darkness, $d(E_0, t_{max}, r)$, becomes a function of only E_0/r. Thus, Eq. (9) leads one to the following similarity relation on the maximum spot darkness of two different energies E_0 and aE_0 as

$$D_{max}(aE_0, aR) = D_{max}(E_0, R). \tag{12}$$

This means that the spot darkness at the shower maximum is a function of only E_0/R, i.e.,

$$D_{max}(E_0, R) = f(E_0/R). \tag{13}$$

3-2 *Numerical evaluation of spot darkness*

Numerical values of the spot darkness was calculated by a computer using the numerical results of the lateral distribution function of an electron shower given by Nishimura.[6] For a set of values of the parameters in the characteristic curve, Eq. (3), we assumed $D_0=7.0$ and $\alpha=3.0$, which correspond to a typical case of N-type X-ray film. Calculation shows that a change of magnitude of parameter α, even with one order of magnitude, causes only a constant shift of transition curves in the spot darkness keeping their relative magnitude as they are. This is because a main contribution to the integration is from the peripheral region of the dark spot where the characteristic curve Eq. (3) can be approximated by a linear relation,

$$D = \alpha\rho D_0 . \tag{14}$$

The numerical results are obtained for various energies E_0, depths t and slit radius R, which cover regions necessary for the practical purpose of the experiment. Examples of calculated transition curves of the spot darkness are shown in Fig. 4. Interpolating values of $D(E_0, t, r)$ with the transition curve, one can obtain the maximum value $D_{max}(E_0, R)$ for a given value of energy and of slit radius. The numerical results on $D_{max}(E_0, R)$ can be represented by the following simple relation,

$$D_{max}(E_0, R) \propto (E_0/R)^{\beta} \tag{15}$$

with

$$\beta = 0.85,$$

which is consistent with the argument presented above.

The above relation (15) can be also obtained analytically under the following approximation:

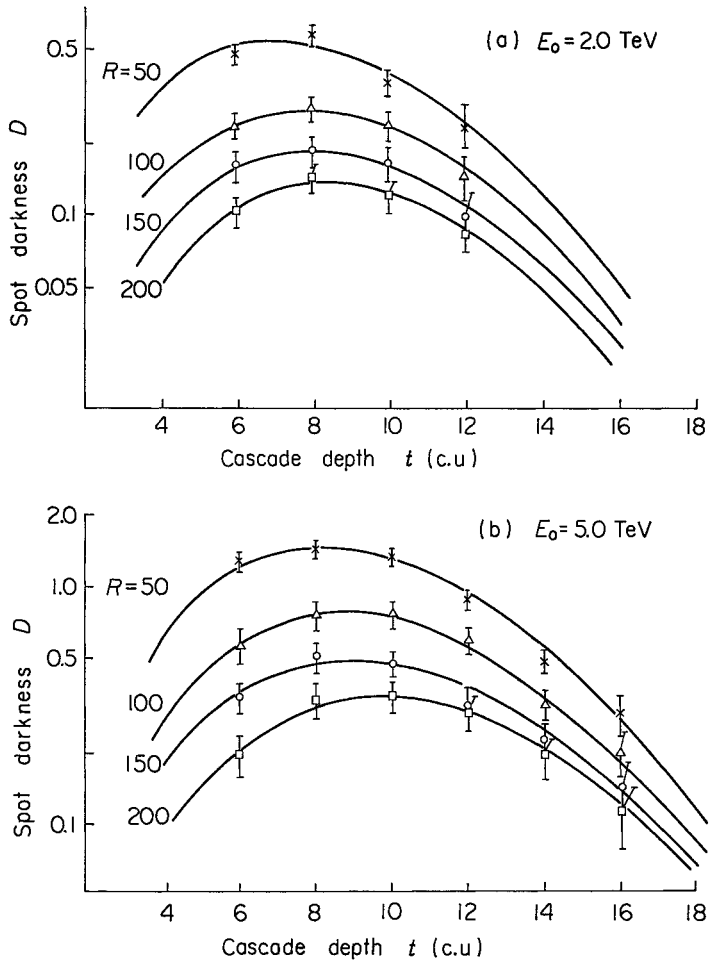

Fig. 4. Transition curves of spot darkness for various sizes of slit, 50, 100, 150 and 200 μm for shower energy E_0=2.0 TeV (a) and E_0=5.0 TeV (b). Full lines present results of the theoretical calculation.

(1) lateral distribution function of electrons at the shower maximum, $s=1$, near the shower axis as

$$\rho(E_0, r, s=1)=c(E_0)/r,$$

(2) the darkness is proportional to the electron density ρ as in Eq. (14),

$$D=\alpha\rho D_0 .$$

Then one can execute the integration in Eq. (9) and obtain the following expression as the maxmium spot darkness,

$$D_{\max}(E_0, R) = -\log[(\alpha c(E_0)/R)\{1-\alpha c(E_0)/R\} + (\alpha c(E_0)/R)^2 E_i(\alpha c(E_0)/R)], \quad (16)$$

where $E_i(x)$ is an exponential integral function. From this expression, it is easily verified that $D_{\max}(E_0, R)$ has the following approximate expression, $D_{\max}(E_0, R) \propto (E_0/R)^{\beta}$ with $\beta=0.85$, over a wide range of value of the parameter $\alpha c(E_0)/R$ from 0.01 to 1.0. The quantity $\alpha c(E_0)/R$ corresponds to an average number of electrons penetrating a single silver-halide crystal, at distance R from the shower center.

3-3 *Measurement on spot darkness*

In the present study 47 electron shower events are selected from the shower events analyzed in Chamber 11. They are listed in Table II. Energy of these events were determined by the track counting method. They cover from $E_0=1.0$ TeV up to 13.0 TeV. The photometry measurement was made with various slit radii, $R=50$, 100, 150 and 200 μm, at various depths where one recognizes a spot of the concerned shower in the X-ray film. Then one constructs the transition curve and estimates the maximum value of the spot darkness for every case. Figure 4 shows examples of the transition curve with various slit sizes and Fig. 5 with various energies. The theoretical curves are drawn together in the same figures for comparison.

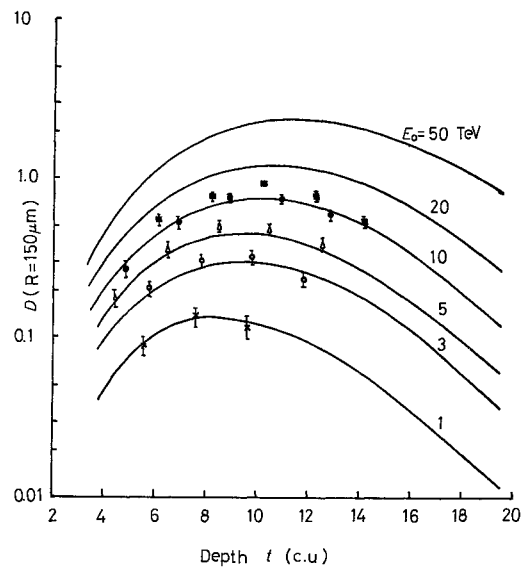

Fig. 5. Transition curves of spot darkness with slit radius $R=150$ μm calculated from shower theory. Experimental data are also plotted.

Now an experimental check is made on the similarity relation which states that the maximum spot darkness $D_{\max}(E_0, R)$ is a function of only (E_0/R). For this purpose, all the data of the maximum spot darkness of an electron shower with various energies are plotted together as a function of slit radius R after applying a scale change of the slit radius R into (5 TeV/E_0)R. This is to make a similarity transformation to a case of electron shower with fixed energy, 5 TeV. The results, given in Fig. 6, show that the experimental points distribute along a single straight line which is expressed by

$$D_{\max}(E_0, R) \propto (R/E_0)^{-\beta} \tag{17}$$

with

$$\beta = 0.85 \pm 0.05.$$

This result is in agreement with the theoretical consideration on the similarity law of an electron shower and also results of the numerical calculations presented above.

The fluctuation of experimental points is not negligible in the region of slit radius smaller than 100 μm as observed in Fig. 6. A part of the fluctuation comes from the effect of the inclination of the shower which will be discussed later. The error in our experiment is estimated to be about 10% for a case with slit radius greater than 100 μm as is seen from the spread of the experimental points in Fig. 6.

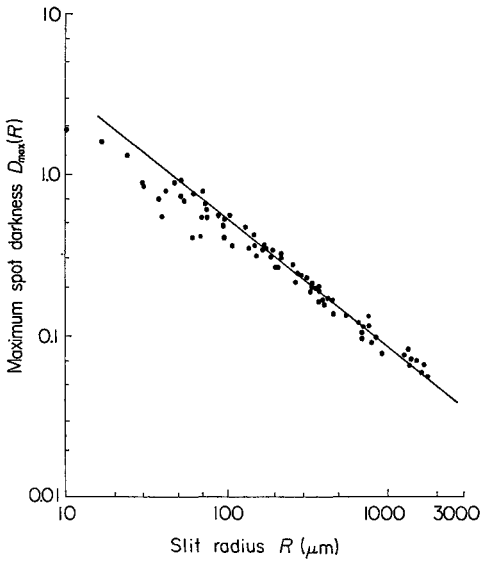

Fig. 6. Dependence of maximum darkness, $D_{\max}$, of shower spot on slit radius, R, for γ-ray showers. Data are normalized to case of $E_0 = 5$ TeV. The solid line shows relation, $D_{\max} \propto E_0^{0.85}$.

3-4 *Energy calibration*

With use of a general argument on the electron shower theory, the results on relation between spot darkness $D_{\max}$ and the slit size R give us the following relation between the spot darkness $D_{\max}$ and the shower energy E_0,

$$D_{\max}(E_0, R_0) \propto E_0^{\beta} \tag{18}$$

with

$$\beta = 0.85 \pm 0.05,$$

where $D_{\max}(E_0, R_0)$ is obtained for a fixed radius, R_0, of the slit.

This relation is examined directly by measurement of the maximum spot darkness with a fixed slit (150 μm radius) for electron shower events with various energies which are determined by the track counting method. Twenty-seven electron showers are selected from Chamber 11, listed in Table II, and 22 showers from Chamber 12 and Chamber 13, listed in Table III. Experimental result is presented in Fig. 7 and it shows the agreement with Eq. (18).

Table II. List of single electron showers. These are selected from Chamber 11, and used to study dependence of the maximum spot darkness on size of slit and relation of the maximum spot darkness and shower energy. The results are presented in Fig. 6 and Fig. 7, respectively. The energies of showers are determined by the track counting method.

(25 events)

Event No.	Zenith angle $m=\tan\theta$	$(E_0)_{count}$ (TeV)	D_{max} (150 μm)	Starting point (c. u)
Chamber 11				
Block 2				
No. 4	0.20	2.3	0.19	4
No. 5	0.16	3.2	0.32	4
No. 6	0.51	2.0	0.20	4
No. 11	0.73	4.2	0.45	4
No. 13	0.41	4.3	0.50	6
No. 21	1.07	13.0	1.00	4
No. 38	0.70	3.2	0.28	4
Block 5				
No. 1	0.35	4.0	0.37	5
No. 21	0.88	7.0	0.66	6
Block 6				
No. 10	0.40	1.0	0.11	6
No. 14	0.60	1.3	0.15	6
No. 17	0.60	1.0	0.11	8
No. 19	0.35	1.8	0.19	8
No. 24	0.52	1.8	0.14	8
No. 26	0.34	1.4	0.12	6
No. 34	0.10	1.6	0.17	6
Block 12				
No. 21	0.30	3.8	0.36	8
No. 26	0.45	2.7	0.29	10
No. 34	0.20	4.5	0.50	6
No. 43	0.20	1.4	0.16	6
Block 13				
No. 5	0.37	5.8	0.48	6
No. 53	0.23	3.0	0.26	8
Block 18				
No. 10	0.50	4.3	0.39	4
No. 37	0.38	1.6	0.39	8
No. 82	0.25	3.2	0.31	8

Table III. List of single electron showers. These are selected from Chambers 12 and 13, and used to study the relation of the maximum spot darkness and shower energy illustrated in Fig. 7. The energies of showers are determined by the track counting method.

(22 events)

Event No.	Zenith angle $m=\tan\theta$	$(E_0)_{count}$ (TeV)	D_{max} (150 μm)	Starting point (c. u)
Chamber 12				
Block 1				
No. 1	0.28	1.6	0.18	8
No. 4	0.32	1.2	0.16	6
No. 35	0.17	3.2	0.32	8
Block 2				
No. 3	0.07	1.9	0.18	6
Block 6				
No. 19	0.08	7.3	0.68	8
Block 8				
No. 3	0.08	2.8	0.20	6
No. 4	0.12	5.4	0.50	8
Block 9				
No. 29	0.10	2.0	0.20	8
No. 30	0.08	5.0	0.50	8
Chamber 13				
Block 47				
No. 11	0.27	2.2	0.21	6
No. 15	0.21	2.4	0.23	6
No. 38	0.16	2.1	0.23	6
No. 73	0.19	4.0	0.39	10
Block 48				
No. 4	0.16	9.6	0.83	6
No. 5	0.15	5.6	0.50	6
No. 6	0.20	3.6	0.46	6
No. 7	0.21	3.5	0.38	6
No. 12	0.19	4.0	0.39	8
Block 49				
No. 1	0.60	14.0	1.13	6
No. 8	0.25	1.0	0.12	6
No. 9	0.13	1.4	0.16	6
No. 10	0.30	1.2	0.14	6

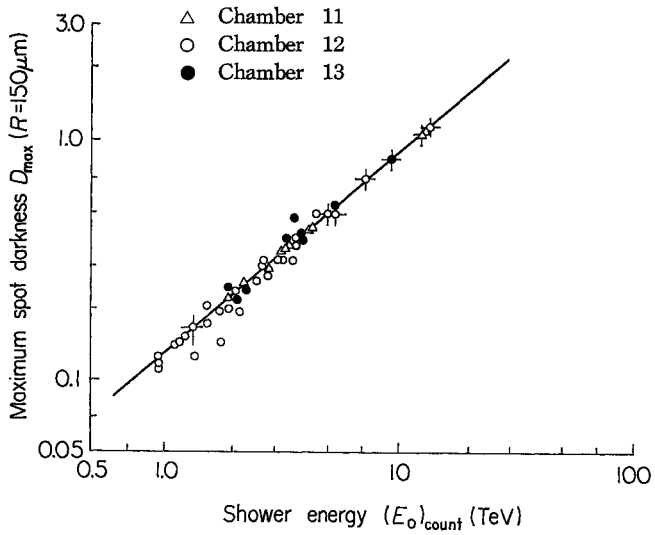

Fig. 7. Correlation of the maximum spot darkness D_{max} with the shower energy measured by track counting, $(E_0)_{count}$.

3-5 *Optimum condition on radius of slit*

In order to determine the optimum size, R_0, of the slit in the photometric measurement, one has to take into account the following three points:

1) Since grain cross-section in N-type film after development is very large (more than 30 times greater than that of ET7A nuclear emulsion), the slit radius must be large enough to eliminate fluctuation caused by the granular structure.

2) As the number of electrons increases with the shower energy, an effect of saturation of the grain density near the shower axis must be taken into account. For example, in the case of shower energy of 10^{13} eV, the mean track density of electrons in a circle of radius 50 μm is about 10^7 electrons/cm^2. The size, R_0, should be greater than a certain size to avoid the saturation effect.

3) The X-ray film has a sensitive emulsion layer on both sides of its acetate base of 200 μm thick. Two spots on both sides by a shower with zenith angle θ are relatively distanced by 230 $\tan\theta$ μm. Thus we must fix the radius of slit to minimize the effect of the two spots.

The effects (1) and (2) can be avoided by choosing the slit size larger than the grain cross-section size and the size of the completely opaque area of the spot, respectively. But it is not advisable to enlarge the slit size extremely because the signal-noise ratio decreases. An essential point for determination of the slit size lies in the condition (3).

Let us consider a relation between inclination of the shower and the slit size. Figures 8(a) and (b) show an effect of the existence of double spot

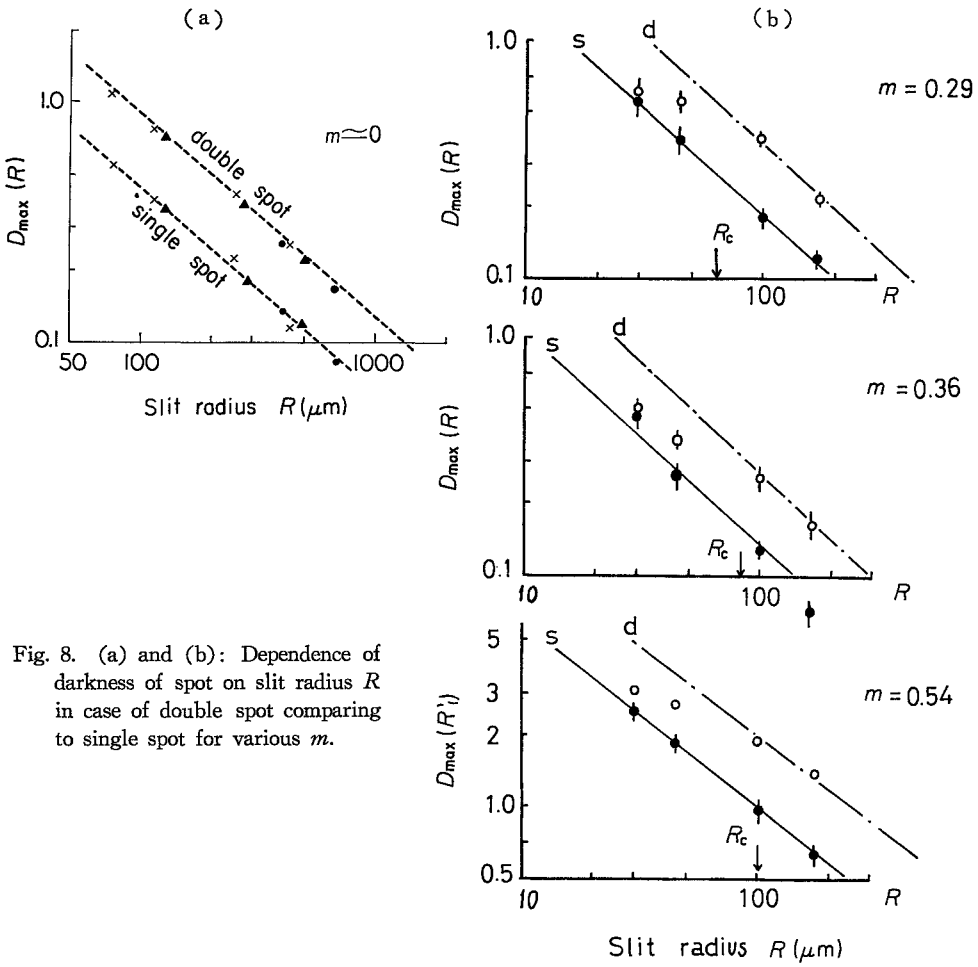

Fig. 8. (a) and (b): Dependence of darkness of spot on slit radius R in case of double spot comparing to single spot for various m.

on both sides, comparing the spot darkness in a double layered X-ray film with that in a single layered film for the same shower. All of the showers plotted in Fig. 8(a) has zenith angle $m=\tan\theta\sim 0$, therefore darkness of the double spot is just twice larger than that of single one for every slit size. In the case of $m\gtrsim 0.3$, as is shown in Fig. 8(b), the same simple relation holds at the larger slit size while a deviation is observed as the slit size reduces. Let us put R_c as the critical slit size where the deviation begins to be appreciable. To obtain a relation between inclination of a shower, m, and the critical slit size R_c, the measurements are performed on the events with wide range of energy and various inclination, and the result is shown in Fig. 9. As can be seen in Fig. 9, R_c increases with the inclination m.

Almost all of showers observed in the emulsion chambers exposed on Mt. Norikura and Mt. Chacaltaya have zenith angles smaller than $m<1.0$. Therefore, we can measure the spot darkness without the effect of shower

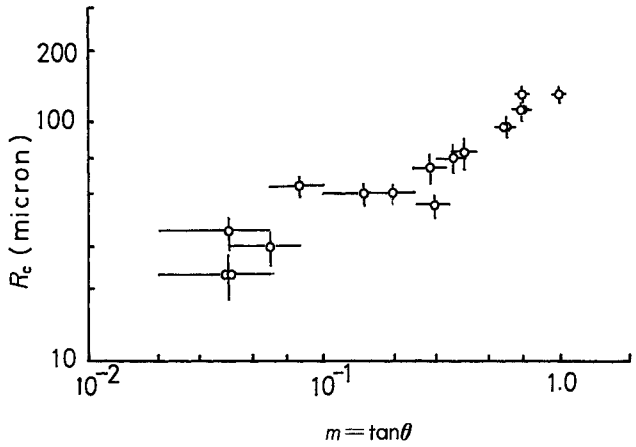

Fig. 9. Relation between shower inclination $m=\tan\theta$ and critical slit radius R_c.

inclination, if we use the slit size R larger than 150 μm. The routine measurement by the micro-densitometer is performed with the slit size R_0 $=150$ μm in our experiment. Details about numerical estimation on this effect are shown in Appendix 2.

§4. Energy determination of Pb-jet shower

Pb-jet shower is a high energy nuclear interaction produced locally in the emulsion chamber itself and is observed as a composite electron showers originated from a number of γ-rays coming from decay of π^0-mesons produced in the nuclear interaction. Therefore, longitudinal and lateral development of the Pb-jet shower will be different from an electron shower of a single incident γ-ray or electron.

4-1 *The similarity relation for Pb-jet shower*

It is well known that the lateral distribution of particles of an electron shower of a single incident γ-ray or electron has a similarity relation on its incident energy E_0 and the lateral distance r from the shower center. Expressing by $\rho(E_0, r, t)$ the particle density of the electron shower, one has

$$\rho(aE_0, r/a, t)=a^2\rho(E_0, r, t). \tag{19}$$

Let us consider a case of Pb-jet shower, i.e., a composite shower generated by a local nuclear interaction in the chamber. Since γ-rays produced in a nuclear interaction has a constant transverse momentum in the average of about a hundred MeV/c and multiplicity of the γ-rays increases with the interaction energy, one expects that lateral distribution of the Pb-jet shower will have generally

$$\rho_{\mathrm{Pb}}(a\sum E_\gamma, r/a, t)\leq a^2\rho_{\mathrm{Pb}}(\sum E_\gamma, r, t) \tag{20}$$

with

$$a\geq 1,$$

where $\sum E_\gamma$ is the energy sum of all γ-rays produced in the interaction and t is the depth meaured from the interaction point.

Through the Japan-Brazil collaboration experiment, one knows now that the main process of multiple production of mesons in the concerned energy region is emission of the H-quantum,—an elemental fire-ball of rest-energy of $\sim$2.4 GeV proposed by Hasegawa in 1961.[7),8)] According to the H-quantum theory, the jet shower is a phenomenon of emission of several H-quanta with different velocities. From this point of view, one concludes that the main part of the Pb-jet shower is from contribution of the first H-quantum, and contributions of the second and later H-quanta with smaller velocities can be neglected. In this approximation, one finds the following simple property of the Pb-jet shower.

Since the nuclear interaction is now represented by a single H-quantum, the properties of which is independent on energy of the interaction, difference of Pb-jet showers with different energy is caused only by a kinematical effect of motion of the produced H-quantum. Therefore, one has again the similarity relation such as

$$\rho_{\mathrm{Pb}}(a\sum E_\gamma, r/a, t)=a^2\rho_{\mathrm{Pb}}(\sum E_\gamma, r, t), \tag{21}$$

just the same as for pure electron showers. It means that the density distribution can be described by the two parameters, $(\sum E_\gamma)\cdot r$, and t. If one restricts oneself to nuclear effect on the lateral spread of shower particles, one finds immediately that it is described by a single relation,

$$\frac{(\sum E_\gamma)\cdot r}{t}\sim r_{\mathrm{H}}\cdot\tan\frac{\theta^*}{2}, \tag{22}$$

where θ^* is an angle in the c.m. system. $\mathfrak{M}_\gamma$ is γ-ray mass of a H-quantum, given as 1.3 ± 0.2 GeV.[8)] Thus one sees that $(\sum E_\gamma)\cdot r/t\sim r_{\mathrm{H}}$ corresponds to a half angle, $\theta^*=90°$, of the concerned H-quantum rest system. Then a lateral distance given as

$$r_c\sim\frac{tr_{\mathrm{H}}}{\sum E_\gamma}, \tag{23}$$

is a characteristic distance, because the nuclear effect will be confined mostly in the region $r\lesssim r_c$ and the lateral distribution of the Pb-jet shower will be more or less of the same form as that of a single electron shower in the outside region, $r\gtrsim r_c$. Further detailed studies on the lateral distribution of the Pb-jet shower are given in Appendix 3.

4-2 *Counting method on Pb-jet showers*

A study of calibration of energy determination by the track counting method on Pb-jet showers was made by Dake.[9] Instead of making the similarity consideration, he constructed a number of model Pb-jet showers with the angular distribution data of jet showers of the ICEF experiment and an energy estimation by the constant p_T rule. He showed that one can determine the energy of Pb-jet shower with the same calibration curve as for the single electron shower when the track counting method is applied using a circular area of radius $R=70\,\mu$m or larger. Since in his model Pb-jets have energies of about $\sum E_\gamma \sim 2$ TeV, one finds that a characteristic radius in his case is $r_c \sim 5\text{ cm} \times 1.3\text{ GeV}/2\text{ TeV} \sim 33\,\mu$m. Thus one sees that the radius of $70\,\mu$m is large enough to eliminate an effect of lateral spread due to the nuclear interaction.

Lateral distributions of electrons in Pb-jet showers were experimentally studied by the track counting method. Three Pb-jet showers are taken for the purpose and the track density distribution was measured for each of them. Figure 10 gives their composite density distribution at the shower maximum after normalizing the experimental data to $\sum E_\gamma = 1$ TeV by application of the similarity relation (23). We presented in the same figure the result of theoretical calculation given in Appendix 3. Here one sees that the experimental data are consistent with the similarity relation and also with the theoretical calculation. The lateral distribution of Pb-jet shower shows a characteristic flatness near the shower center as compared to a case of a single electron shower. The characteristic radius is $r_c \sim 65\,\mu$m for $\sum E_\gamma = 1$ TeV.

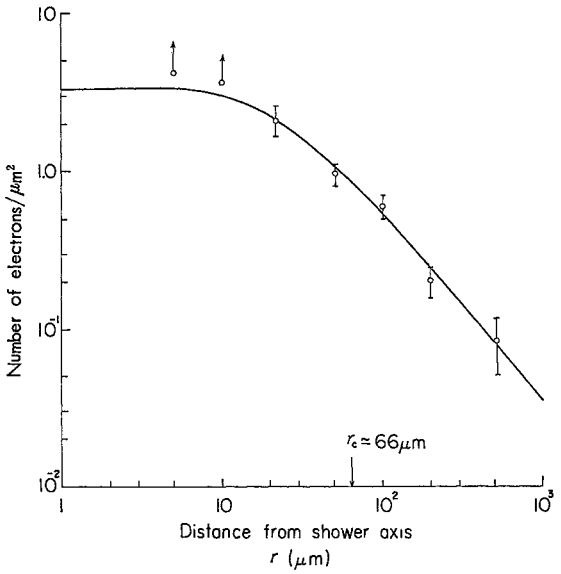

Fig. 10. Lateral distribution of electrons of Pb-jet shower with energy $\sum E_\gamma = 10^{12}$ eV at shower maximum. Solid line shows the calculated results.

4-3 *Photometry of Pb-jet shower*

Let us discuss a spot darkness of the Pb-jet shower in the same point of view. To avoid the effect of the inclination of a shower, we selected the events

only with $m<0.3$. The darkness $D(\sum E_\gamma, R)$ was measured with various slit radii for 23 events listed in Table IV. Normalizing the results to a standard shower with $\sum E_\gamma = 5.0$ TeV applying the similarity relation in the same way as for single electron showers in Eq. (12), the experimental values of the spot darkness at the shower maximum $D_{max}(\sum E_\gamma = 5\,\text{TeV}, R)$ are plotted in Fig. 11 as a function of the slit radius R. A straight line in the figure represents a power law, $D_{max} \propto R^{-0.85}$, which gives a good fit to data of single electron showers as shown in Fig. 6. One sees their agreement except in a region of very small radius.

From these qualitative results, one may conclude that the energy determination of Pb-jet showers by the photometry measurement can be done by

Table IV. List of Pb-jet showers. These are selected from Chamber 11, and used to study dependence of the maximum spot darkness on size of slit and the relation of the maximum spot darkness and shower energy. The results are presented in Fig. 9 and Fig. 11, respectively.

(23 events)

Event No.	Zenith angle $m=\tan\theta$	$(E_0)_{count}$ (TeV)	D_{max} (150 μm)	Starting point (c.u.)
Block 2				
No. 73	0.04	2.1	0.20	18
No. 95	0.04	5.5	0.46	28
No. 103	0.06	3.5	0.30	32
Block 7				
No. 3	0.50	2.7	0.26	20
No. 20	0.04	3.5	0.32	48
No. 56	0.08	2.0	0.20	22
No. 65	0.84	3.7	0.35	28
No. 75	0.20	1.8	0.18	14
No. 102	0.18	2.3	0.24	44
No. 157	0.60	1.9	0.18	22
No. 158	0.60	3.4	0.33	20
No. 113	0.30	10.5	0.75	36
Block 6				
No. 88	0.20	2.5	0.27	44
No. 89	0.60	3.0	0.31	44
No. 91	0.40	1.5	0.18	48
No. 92	0.40	2.0	0.22	52
Block 13				
No. 22	0.28	4.7	0.42	44
No. 24	0.28	3.3	0.30	40
No. 25	0.28	16.5	1.15	40
No. 62	0.41	3.0	0.26	14
No. 73	0.20	2.7	0.26	24
No. 75	0.90	3.5	0.34	24
No. 95	0.28	6.7	0.52	48

using the same calibration curve for single electron showers when the slit size is larger than the characteristic radius given by Eq. (23). Figure 12 presents experimental results on the maximum spot darkness $D_{max}(R_0)$ and the estimated energy $\sum E_\gamma$ by the track counting method. The slit radius is fixed as $R_0 = 150\,\mu$m. A straight line in Fig. 12 is a calibration curve for single electron showers. Its agreement with experimental data confirms the above conclusion.

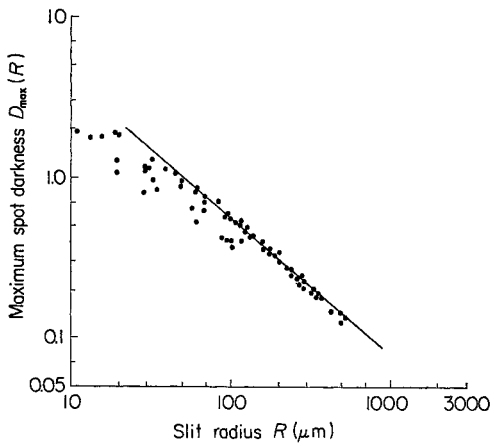

Fig. 11. Dependence of maximum darkness, D_{max}, of shower spot on slit radius, R, for Pb-jet shower. Data are normalized to case of $\sum E_\gamma = 5$ TeV. The solid line shows relation, $D_{max} \propto E_0^{0.85}$.

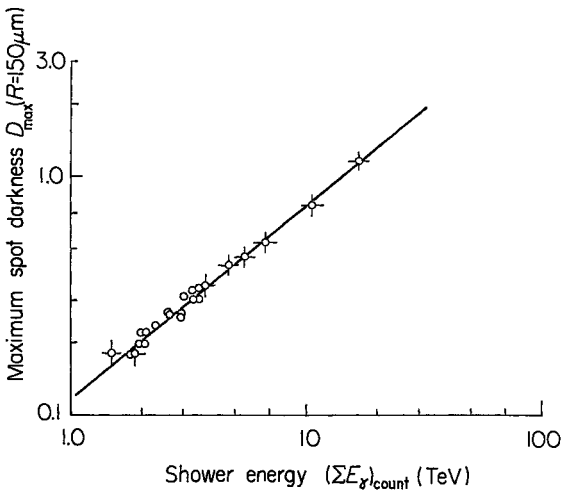

Fig. 12. Correlation of the maximum spot darkness D_{max} and the shower energy $(\sum E_\gamma)_{count}$ of Pb-jet shower determined by track counting.

§5. Conclusion

The present work established the photometric method with X-ray films for energy determination of cosmic-ray showers in the emulsion chamber. The procedure of energy determination is summarized as follows:

1. Darkness of the shower spot is defined as

$$D(\text{net}) = D(\text{ob}) - D(\text{bg}).$$

The radius of slit for measurement of the darkness is fixed ($R_0=150\ \mu$m) in our experiment.

2. Measuring the darkness of shower spot in each cascade depth and interpolating these values with help of the calculated transition curve, the maximum spot darkness, D_{max}, is determined.

3. A calibration curve between D_{max} and energy E_0 is constructed for each emulsion chamber of different exposure. One picks up a few tens of pure electron showers, and their energies are determined by the track counting method. The relation of D_{max} and E_0 is obtained from the measured energy E_0 and the maximum spot darkness D_{max} of these showers. It should consist of a relation $D_{max}\propto E^{0.85}$.

4. Using the calibration curve between E_0 and D_{max}, one is able to determine energy of any electron shower in the chamber by measuring its maximum spot darkness.

5. Effect of the inclination of showers on the measurement of spot darkness is evaluated and is shown negligible, if the zenith angle is smaller than 45°. If zenith angle is greater than 45°, one should apply the correction factor given in Appendix 2.

6. Experimental error of the spot darkness measurement is about 10%, which gives an error of about 15% in the energy determination.

The lateral distribution of electrons in a Pb-jet shower with interaction energy $\sum E_\gamma \geq 2$ TeV is approximately equal to that in a single electron shower with the same energy, when one confines oneself in a region of larger distance, $r \geq r_e \approx 33\ \mu$m, from the shower center. Therefore, the same photometric method for energy determination can be applied to Pb-jet showers as for single electron showers.

Acknowledgements

The author would like to express his sincere gratitude to Professor J. Nishimura, Professor Y. Fujimoto, Professor S. Hasegawa, Professor N. Ogita, Professor K. Niu, Professor I. Mito and Dr. T. Taira for their many valuable discussions.

He is indebted to the Brazilian emulsion chamber group under Professor C. M. G. Lattes and the Japanese emulsion chamber group who participated a part of the work and maintained constant interest.

Thanks are also due to Mr. H. Sugimoto for photometric measurement and for valuable advices and to Miss A. Adachi for her assistance in numerical calculation.

Appendix 1

——Background darkness of X-ray films——

Origin of the background darkness of X-ray film can be classified into two categories. One is due to the background radiation which the films received during exposure period and it consists of the soft and hard component of the cosmic-rays and radiation from natural activity. The other is due to the chemical fog and it depends on the condition of manufacturing and processing of the X-ray film. Figure A1-1 shows the photometric darkness of background of N-type and RR-type films in Chamber 11, exposed on Mt. Chacaltaya for about one year. High level of the background near the top of the chamber is considered to be due to soft component of cosmic-rays, and a small increase near the bottom of the chamber will be due to the terrestrial natural activities. For elimination of the background darkness it is necessary to know fluctuation of the background darkness in one sheet of the X-ray film. We measured the photometric darkness, D, at 250 locations randomly sampled in a sheet of N-type and RR-type film, respectively. The experimental distribution of the background darkness normalized their average to $D=1.0$ is shown in Fig. A1-2. A half width of the distribution is 0.05 ± 0.02 for N-type and 0.02 ± 0.01 for RR-type film, respectively.

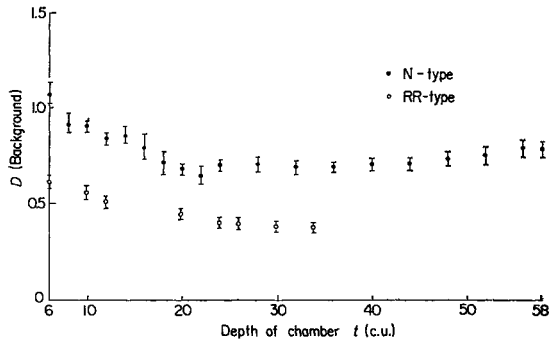

Fig. A1-1. Background darkness of N- and RR-type films in the emulsion chamber which was exposed on Mt. Chacaltaya for about one year.

In order to have higher value of spot darkness in X-ray film, we investigated the effect of the development condition by making artificial spots by irradiation of six different doses of β-rays (with momentum 765 KeV/c from activated $Tl_2^{204}(SO_4)$) on the N-type films and making photometry measurement on the spots. The developing time is varied from 5 to 30 minutes under the standard temperature. Figure A1-3 shows variation of the spot darkness and the background darkness of the film with developing time. As can be seen from Fig. A1-3, the net spot darkness increases at first with the

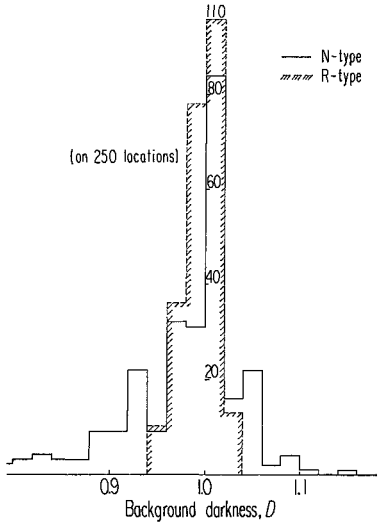

Fig. A1-2. Fluctuation of background darkness on N- and RR-type films. Darkness of background is measured at 250 locations in the same film.

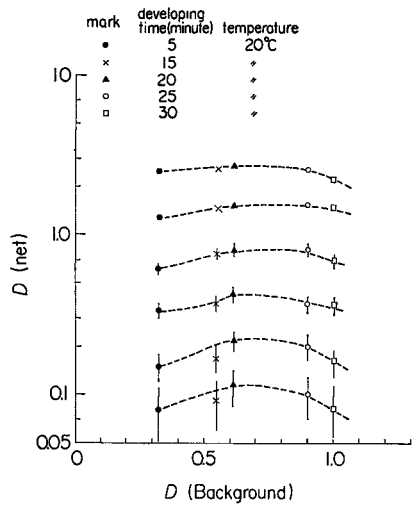

Fig. A1-3. Relation between net darkness of model shower and background darkness of N-type film. The model showers were made by irradiation of β-rays. The development was made at standard temperature 20°C.

development time, and then gradually decreases when the development time becomes too long. This is because the size of grain increases with development time and level of the background darkness increases more rapidly than the spot darkness. This tendency is more remarkable for a spot of a small amount of irradiation, i.e., for a lower value of spot darkness. The developing time in the routine procedure is fixed as about 15 minutes under the standard temperature at 20°C.

Appendix 2

——Zenith angle effect in photometry measurement——

A sheet of X-ray film has two sensitive emulsion layers 30 μm thick on both surfaces of a transparent acetate base film 200 μm thick. A shower produces two spots on both of the layers with the relative lateral displacement,

$$d = 230 \tan\theta \ \mu\text{m},$$

where θ is the zenith angle of the shower. The effect of shower inclination appears in the following three factors:

(1) The relative distance of two spots increases with $\tan\theta$;

(2) density of tracks varies as $\cos\theta$; and

(3) length of shower tracks increases with $\sec\theta$.

Increase of displacement of the two spots generally makes the spot darkness decrease. On the other hand, darkness of a shower spot is proportional to the density of tracks and the length of tracks as well. Since the factors (2) and (3) compensate with each other, their resultant effect of inclination will be negligibly small when the relative displacement of both spots is smaller than the diameter of slit.

The numerical calculation was carried out for two cases. One is the case where the slit center is focused on the middle point of the distance of the two spots, and the other is the case where the slit center is focused on the center of one spot.

The results are illustrated in Fig. A2-1 compared with the case of vertical showers for wide range of energies and zenith angles. The results show the necessary correction factor of darkness of shower spot with inclination to stay within 5% for the case of slit radius $R=150\,\mu$m. This result is confirmed with experimental measurement as described in §3.

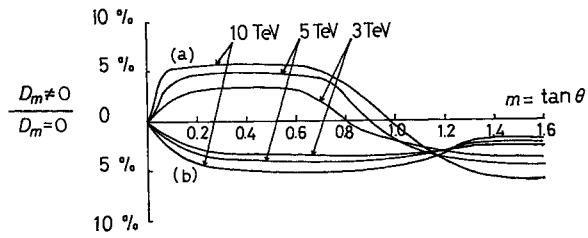

Fig. A2-1. Effect of inclination of electron shower on the darkness: (a) case where the slit center is focused in the center of displacement of two shower spots; (b) case where the slit center is focused on the center of a shower spot either surface or back-face of film.

Appendix 3

——Lateral distribution of electrons in Pb-jet shower——

Let us consider a nuclear interaction of single H-quantum production. One expresses by $\mathfrak{M}_\gamma$ a part of its rest energy given to γ-rays. Then the interaction energy, $\sum E_\gamma$, is determined by

$$\sum E_\gamma = \gamma_H \mathfrak{M}_\gamma, \qquad (A\cdot 3\cdot 1)$$

where γ_H is Lorentz factor of motion of the H-quantum.

Suppose single H-quantum decays isotropically into γ-rays with a constant momentum p^* in its rest system. Angular distribution of the γ-rays is expressed as

$$g(\theta)d\theta = 1/2\, d(\cos\theta^*) = 2\gamma_H^2\theta d\theta/(1+\gamma_H^2\theta^2), \qquad (A\cdot 3\cdot 2)$$

and the energy E_γ of each γ-ray in the laboratory system is given as the following function of its emission angle θ in the same system as

$$E_\gamma = p_\gamma = r_H p^*(1+\cos\theta^*) = 2r_H^2 p^*/(1+r_H^2\theta^2), \qquad (A\cdot 3\cdot 3)$$

where θ^* is the emission angle of γ-ray in the H-quantum rest system.

The lateral distribution of electrons in a Pb-jet shower at the depth t from its starting point, $\rho_{Pb}(r,t)$, can be constructed from the angular distribution function, $g(\theta)$, of constituent γ-rays and the lateral structure function, $\rho(E_\gamma,t,r)$, of shower electrons as

$$\rho_{Pb}(r,t) = \int \rho(E_\gamma(\boldsymbol{r}'), \boldsymbol{r}-\boldsymbol{r}', t) g(\boldsymbol{r}'/t) d\boldsymbol{r}', \qquad (A\cdot 3\cdot 4)$$

where it should be noted that E_γ is a function of variable r' through Eq. (A·3·3) and the relation $r'=\theta t$, as

$$E_\gamma(r') = 2r_H p^*/[1+r_H^2(r'/t)^2]. \qquad (A\cdot 3\cdot 5)$$

Since the functions ρ and g are symmetric in azimuth, the Hankel transformation is applicable as

$$\rho_{Pb}(r,t) = \int J_0(\zeta r)\zeta d\zeta [J_g(\zeta)\cdot J_\rho(\zeta)], \qquad (A\cdot 3\cdot 6)$$

where J_g and J_ρ are the Hankel transformation of g and ρ, and

$$[J_g(\zeta)\cdot J_\rho(\zeta)] = \int g(r,t) J_0(\zeta r) r \left\{ \int \rho(E_\gamma, r', t) J_0(\zeta r') r' dr' \right\} dr$$

cannot be reduced to simple multiplication $J_g \cdot J_\rho$, because of Eq. (A·3·5). The function $\rho(E_\gamma, r, t)$ is given by the three-dimensional shower theory and is expressed as

$$\rho(E_\gamma, r', t) r' dr' = \int (E_\gamma r'/K)^s \Gamma(1+s/2) M(s, -s/2, t) dr'/r' ds, \qquad (A\cdot 3\cdot 7)$$

with the boundary condition corresponding to γ-ray initiation.

Finally, the lateral distribution is described by the following expression,

$$\rho_{Pb}(r,t) = (2r_H p^*/K)^{\bar{s}} (\gamma_H/t)^{-(\bar{s}+1)} \Gamma(1+\bar{s}/2)\Gamma(\bar{s}/2)/\Gamma(1-\bar{s}/2)\Gamma(2+\bar{s}) \times \int_0^\infty J_0(\zeta r) K_{-(\bar{s}+1)}(t\zeta/\gamma_H)\zeta^2 d\zeta, \qquad (A\cdot 3\cdot 8)$$

where $\bar{s}$ is the shower age determined by the saddle point method in integration over s, and $K_{-(\bar{s}+1)}$ is the modified Bessel function of order $-(\bar{s}+1)$.

As can be seen briefly from the above expression, the form of the lateral distribution at shower maximum, $s=1$, is expressed by the function of r_H and β alone,

$$\rho_{\mathrm{Pb}}(r)\propto\gamma_{\mathrm{H}}^{2}\int_{0}^{\infty}J_{0}(\beta x)K_{-(s+1)}(x)x^{2}dx,$$

where $\beta=\gamma_{\mathrm{H}}r/t$ and $x=t\zeta/\gamma_{\mathrm{H}}$, respectively. Now, one sees explicitly that the following similarity relation holds for the lateral distribution of electrons in Pb-jet shower,

$$\rho_{\mathrm{Pb}}(a\sum E_{\gamma}, r/a, t)=a^{2}\rho_{\mathrm{Pb}}(\sum E_{\gamma}, r, t),$$

just similarly to the case of a single γ-ray incident.

The numerical calculation is carried out with the following values:

radiation length in emulsion chamber $=7.5$ mm
scattering constant $K=19.7$ MeV
momentum of γ-ray $p^{*}=200$ MeV$/c$
γ-ray mass of the H-quantum $\mathfrak{M}_{\gamma}=1.3$ GeV.

The distribution at $s=1$ calculated from Eq. (A·3·8) is compared with experimental result in Fig. 10 of §4, where the experimental distribution is normalized for $\sum E_{\gamma}=1.0$ TeV with the similarity relation mentioned above. The calculated distribution of a single electron shower of 1 TeV is also given in the same figure. The distributions at larger distance show the same feature although remarkable difference in the distributions near the axis is recognized.

The above argument on the similarity of Pb-jet shower has a general character, which can be extended to the case with effects of successive interactions as far as the mean free path and the inelasticity are energy-independent. Then the present formalism on the generalized similarity can be applied to more general nuclear cascade phenomena, for example extensive air showers, than the Pb-jet shower.

But one immediately notices that the present experimental information on extensive air showers suggests failure of such generalized similarity relation on $\sum E_{\gamma}$ and r though the evidences are not definite. Thus one is compelled to conjecture that the premise of the similarity law will not hold in such extremely high energy regions of air showers. In fact, the Japan-Brazil collaboration experiment on the A-jet (atmospheric jets) covers the higher energy region, $\sum E_{\gamma}\lesssim 400$ TeV, and it shows the existence of a fire-ball of larger mass —SH-quantum with $\mathfrak{M}_{\gamma}\sim 8$ GeV. There are evidences for a still larger fire-ball with $\mathfrak{M}_{\gamma}\sim 70$ GeV in interactions of $\sum E_{\gamma}=10^{3}\sim 10^{4}$ TeV.[8] Therefore it should be noticed that the present method with the H-quantum model has a limit of validity in the applied energy region. Detailed discussions on extensive air showers and large fire-balls will be made in another paper.

References

1) O. Minakawa, Y. Nishimura, M. Tsuzuki, H. Yamanouchi, H. Aizu, H. Hasegawa, K. Ishii, S. Tokunaga, Y. Fujimoto, S. Hasegawa, J. Nishimura, K. Niu, K. Nishikawa, K. Imaeda and M. Kazuno, Nuovo Cim. Suppl. **11** (1959), 125.

2) J. Nishimura and K. Kamata, Prog. Theor. Phys. Suppl. No. 6 (1958), 93.
3) Japanese Emulsion Chamber Group-M. Akashi, Z. Watanabe, A. Misaki, I. Mito, Y. Oyama, S. Tokunaga, T. Ogata, Y. Tsuneoka, S. Dake, K. Yokoi, S. Hasegawa, J. Nishimura, K. Niu, T. Taira, A. Nishio, Y. Fujimoto and N. Ogita, Prog. Theor. Phys. Suppl. No. 32 (1964), 1.
4) C. M. G. Lattes, C. Q. Orsini, I. G. Pacca, M. T. Cruz, E. Okuno, Y. Fujimoto, S. Hasegawa and K. Yokoi, Nuovo Cim. **33** (1964), 680.
5) T. Yuda, A. Masaike, A. Kusumegi, Y. Murata, I. Ohta and J. Nishimura, Nuovo Cim. **65A** (1970), 205.
6) J. Nishimura, *Handbuch der Physik* (Springer Verlag), 46/II (1967), 1; Prog. Theor. Phys. Suppl. No. 32 (1964), 72.
7) S. Hasegawa, Prog. Theor. Phys. **26** (1961), 151.
8) Japanese-Brazilian Emulsion Chamber Group-M. Akashi, Z. Watanabe, I. Mito, K. Niu, I. Ohta, A. Osawa, T. Taira, J. Nishimura, Y. Fujimoto, S. Hasegawa, K. Kasahara, E. Konishi, T. Shibata, N. Tateyama, N. Ogita, Y. Maeda, K. Yokoi, Y. Tsuneoka, A. Nishio, T. Ogata, M. Hazama, K. Nishikawa, Y. Oyama, S. Dake, C. M. G. Lattes, M. S. M. Mantovani, C. Santos, E. H. Shibuya, A. Turtelli Jr., N. M. Amato, A. M. F. Endler, M. A. B. Bravo and C. Aguirre, "Chacaltaya Emulsion Chamber Experiment", Prog. Theor. Phys. Suppl. No. 47 (1971), 1.
9) S. Dake, Uchusen Kenkyu (mimeographed circular in Japanese), Vol. **7** (1964), 229.

Erratum

Photometric Method in Energy Determination of Cosmic-Ray Showers in Emulsion Chamber

Itaru OHTA

Prog. Theor. Phys. Suppl. No. 47 (1971), 271.

In Fig. 10 on p. 290 the vertical scale should be corrected by one order. That is, the number of electrons/μm^2, 1.0 should read 0.1.